

## Research Note

### Near-surface layer replacement for sparse data: Is interpolation needed?

Sun, Yimin; Verschuur, D.J.; Luo, Yi

**DOI**

[10.1111/1365-2478.12501](https://doi.org/10.1111/1365-2478.12501)

**Publication date**

2017

**Document Version**

Accepted author manuscript

**Published in**

Geophysical Prospecting

## Citation (APA)

Sun, Y., Verschuur, E., & Luo, Y. (2017). Research Note: Near-surface layer replacement for sparse data: Is interpolation needed? *Geophysical Prospecting*, 65(6), 1694-1705. DOI: 10.1111/1365-2478.12501

## Important note

To cite this publication, please use the final published version (if applicable).  
Please check the document version above.

## Copyright

Other than for strictly personal use, it is not permitted to download, forward or distribute the text or part of it, without the consent of the author(s) and/or copyright holder(s), unless the work is under an open content license such as Creative Commons.

## Takedown policy

Please contact us and provide details if you believe this document breaches copyrights.  
We will remove access to the work immediately and investigate your claim.

# **Research Note: Near-Surface Layer Replacement for Sparse Data: is interpolation needed?**

**Yimin Sun<sup>1\*</sup>, Eric Verschuur<sup>2</sup>, Yi Luo<sup>3</sup>**

*1. EXPEC ARC GRC Delft, Aramco Overseas Company B.V., Delft, 2600 GA, The Netherlands.*

*2. Delft University of Technology, Delft, 2600 GA, The Netherlands.*

*3. EXPEC ARC, Saudi Arabian Oil Company, Dhahran, 31311, Saudi Arabia.*

*\* Corresponding author, email: [sun.delft@gmail.com](mailto:sun.delft@gmail.com)*

## **ABSTRACT**

The near-surface is a common challenge faced by land seismic data processing, where often, due to near-surface anomalies, events of interest are obscured. One method to handle this challenge is near-surface layer replacement, which is a wavefield reconstruction process based on downward wavefield extrapolation with the near-surface velocity model and upward wavefield extrapolation with a replacement velocity model. This requires, in theory, that the original wavefield should be densely sampled. In reality, data acquisition is always sparse due to economic reasons, and as a result in the near-surface layer replacement data interpolation should be resorted to. For datasets with near-surface challenges, because of the complex event behavior, a suitable interpolation scheme by itself is a challenging problem, and this in turn makes it difficult to carry out the near-surface layer replacement. In this research note, we first point out that the final objective of the near-surface layer replacement is not to obtain a newly reconstructed wavefield, but to obtain a better final image. Next, based upon this finding, we propose a new thinking, interpolation-free near-surface layer replacement, which can handle complex datasets without any interpolation. Data volume expansion is the key idea, and with its help, the interpolation-free near-surface layer replacement is capable of preserving the valuable information of areas of interest in the original dataset. Two datasets, one 2D synthetic dataset and one 3D field dataset, are used to demonstrate this idea. One conclusion that can be drawn is that an attempt to interpolate data before layer replacement may deteriorate the final image after layer replacement, while the interpolation-free near-surface layer replacement preserves all image details in the subsurface.

## **KEYWORDS**

CFP, Imaging, Near-surface, Layer replacement, Redatuming

## INTRODUCTION

The complex near-surface is a common problem faced by land seismic data processing and imaging. In areas such as deserts, mountains and glacial environments, there often exist complex near-surface density and velocity anomalies which distort reflected seismic waves from deeper areas of interest (Keho and Kelamis, 2012). Some methods have been proposed to handle this challenge (Taner et al., 1974; Marsden, 1993a,b,c), and among them near-surface layer replacement (NSLR) is a classic one (Berryhill, 1979, 1984; Yilmaz and Lucas, 1986). In NSLR, the actual near-surface velocity model and a replacement near-surface velocity model are estimated first, and then based upon these models NSLR can be carried out. Wave-equation datuming (Berryhill, 1984) through the Rayleigh integral (Gisolf and Verschuur, 2010) is required for NSLR, which implies that a densely sampled surface wavefield is needed (Bevc, 1997; Kelamis et al., 2002). Due to real data acquisition limits, almost all 3D real field datasets are sparse in at least two out of the four spatial coordinates, source x, source y, receiver x and receiver y. Therefore, to correctly implement the Rayleigh integral, some approximations or data interpolation is always necessary. Several approaches have been proposed: Tegtmeier et al. (2004) proposed a 3D data mapping procedure based on kinematic attributes of the near-surface propagation operators; Alkhalifa and Bagaini (2006) proposed a 3D redatuming procedure under the straight rays assumption; Lokshantov and Lotsberg (2009) showed an approximate 3D redatuming of common azimuth gathers, based upon the principles of Biondi and Palacharla (1996).

For sparse data, should accurate interpolation be achieved, NSLR indeed is capable of fixing wavefront distortion from near-surface anomalies. However, as we pointed out previously (Sun et al., 2014), most current interpolation schemes are based upon the fact that the input dataset can be represented sparsely in a certain transformation domain, and the sparser it is in such a domain, the more accurate the final interpolated result can be. Unfortunately, for datasets with a complex

near-surface, this requirement is extremely hard to meet, which makes interpolation for such datasets a challenge by itself. In this situation, inaccurate interpolation in NSLR leads to uncertainties in the final dataset, hence all further manipulations based upon this NSLR processed dataset will be compromised.

Because this interpolation challenge seems to be unsolvable for the time being, it would be preferable if NSLR can be done without interpolation. Moreover, we need to bear in mind that in seismic data processing the final objective is to obtain a better subsurface image. Since seismic data acquisition is designed to acquire enough information to do migration for areas of interest, this means that if the acquisition is not badly compromised and all the original information in the dataset can be preserved somehow in NSLR, then accurate interpolation may not be needed at all! Using this insight as a starting point, we propose a new thinking named interpolation-free near-surface layer replacement (IFNSLR), which requires no interpolation scheme but can still fix near-surface distortions for events of interest.

## **NEAR-SURFACE LAYER REPLACEMENT AND MIGRATION**

Seismic methods are used to image geological structures in the subsurface of the earth (Waters, 1987). To this end, in seismic exploration, the data acquisition scheme is designed to acquire enough information of the subsurface for imaging, which is normally done using migration. In theory, migration is a sparse manipulation, for instance 3D migration maps 5-dimensional data,  $(s_x, s_y, g_x, g_y, t)$ , into a 3-dimensional image,  $(x, y, z)$ . This is the main reason why almost all field datasets do not have to be densely sampled in all spatial directions: an acceptable migration result can be obtained as long as all subsurface points are covered by data acquisition.

Compared to migration, the situation for NSLR is different. NSLR is a wavefield reconstruction method, and it is based on wave propagation theory. The Rayleigh integral is the workhorse in NSLR, so in theory the wavefield has to be densely sampled. In other words, unlike migration,

NSLR is a dense manipulation, and for 3D NSLR, it maps 5-dimensional data,  $(s_x, s_y, g_x, g_y, t)$ , into new 5-dimensional data,  $(s_x, s_y, g_x, g_y, t)$ . Due to this reason, interpolation is always needed in NSLR should the input data be sparse in order to make it well sampled. Note that the term “interpolation” is actually not clearly defined in the field of seismic data processing, and our understanding is that interpolation means adding new information to a dataset in order to predict data at places not being measured. Although normally new information creates extra traces, it does not mean that any manipulation that creates data at new trace locations should be labeled as “interpolation” because new information might not be brought in.

As we pointed out above, for the purpose of migration dense sampling is not necessary, so this gives us a hint that as long as we can keep all the information in the original dataset in the NSLR process, a dense input dataset then should not be required at all! Once this information preservation is fulfilled, then it may be possible to bypass the interpolation challenge for complex data. In the next section the idea of data volume expansion (DVE) will be introduced, which can fulfill the job of information preservation in NSLR.

## **DATA VOLUME EXPANSION AND INTERPOLATION-FREE NEAR-SURFACE LAYER REPLACEMENT**

The mathematical expressions for forward wavefield extrapolation and backward wavefield extrapolation used in NSLR can be written down as follows (Gisolf and Verschuur, 2010)

$$p(\vec{r}_A, t) \approx \frac{z_A}{2\pi} \iint_{\Sigma} \frac{1}{\Delta r^3} \left\{ p[x, y, 0; t - \Delta t(x, y, 0)] + \Delta t(x, y, 0) \frac{\partial}{\partial t} p[x, y, 0; t - \Delta t(x, y, 0)] \right\} ds \quad (1)$$

$$p(\vec{r}_A, t) \approx \frac{z_A}{2\pi} \iint_{\Sigma} \frac{1}{\Delta r^3} \left\{ p[x, y, z_0; t + \Delta t(x, y, z_0)] - \Delta t(x, y, z_0) \frac{\partial}{\partial t} p[x, y, z_0; t + \Delta t(x, y, z_0)] \right\} ds \quad (2)$$

where  $\Delta t$  is the wave propagation time from point  $(x, y, 0)$  or  $(x, y, z_0)$  on the source plane to  $\vec{r}_A$  on the target plane,  $z_A$  is the vertical distance between the source plane and the target plane,  $\Sigma$  covers the whole source plane but usually can be approximated by the Fresnel zone.

Equations 1 and 2 are information conserving. This means if wave propagation is done exactly in this manner, then all subsurface structure information (reflection coefficients) in the original wavefield (or traces) will be kept, although the wavefield is altered somehow. However, according to these two equations, for sparse data, this information conservation comes with a price of data volume expansion (DVE): after one backward wave propagation with the original velocity and one forward wave propagation with a different replacement velocity, the original trace will become a bunch of new traces.

Based upon the discussions above, we now propose the detailed workflow of interpolation-free near-surface layer replacement (IFNSLR) as follows: 1) sort the input sparse dataset into shot gathers, 2) with the original velocity of the near-surface layer, backward extrapolate receivers to a dense receiver grid on the datum, 3) sort the intermediate dataset into receiver gathers, 4) with the original velocity, backward extrapolate sources to a dense source grid on the datum, 5) sort the intermediate dataset into shot gathers, 6) with the replacement velocity, forward extrapolate receivers to a dense receiver grid on the surface, 7) sort the intermediate dataset into receiver gathers, and 8) with the replacement velocity, forward extrapolate sources to a dense source grid on the surface. After IFNSLR, the final dataset is data-volume expanded with new traces emerging on both source and receiver side.

The idea behind IFNSLR is that by allowing the wavefield to propagate in a dense data grid at each extrapolation step, the final data volume will be expanded but none of the original information is lost. However, if a sub-optimal data interpolation process is carried out, these approximated traces will be mixed with the original traces, creating artefacts in the final image. This is demonstrated on both a 2D and a 3D example below.



## EXAMPLES

### 2D Synthetic Example: IFNSLR for Migration

The 2D synthetic model is shown in Figure 1a. Above  $z = 500 \text{ m}$  there are some complex near-surface anomalies, and at  $z = 2500 \text{ m}$  there is a flat reflector. Around  $z = 900 \text{ m}$  and  $z = 1500 \text{ m}$  there exist some regular reflection structures. In this 2D synthetic model, velocity and density are related via Gardner's Equation (Gardner, 1974). Forward modeling parameters include a surface range in the  $x$  direction of  $10 \text{ km}$  with dense receiver sampling of  $25 \text{ m}$  with sparse source sampling of  $200 \text{ m}$ , a simulation time window of  $2.5 \text{ s}$  and a source wavelet over a frequency range up to  $60 \text{ Hz}$ . Absorbing boundaries are used in the forward simulation. Due to the presence of residual reflections from the boundaries an  $f$ - $k$  filter is applied in order to remove these artefacts. The migration scheme used in this paper is one-way wave equation migration (Berkhout, 1982) using optimized space-frequency domain convolution operators (Thorbecke et al., 2004), and migration is done up to a depth of  $3500 \text{ m}$ .

For comparison purposes, we use the true velocity model (Figure 1a) to migrate the forward modeled sparse data, and the final migrated image is shown in Figure 2a. As we mentioned before, data acquisition is usually designed to make sure that enough information is available for the areas of interest for migration. Now, if we look at our migrated image in Figure 2a, indeed our data acquisition scheme meets this requirement, and all structures below  $z = 500 \text{ m}$  are well imaged, even though the modeled data are sparsely sampled on the source side. Figure 2b shows the central shot gather, and the arrow points to the reflection event from the flat reflector at  $z = 2500 \text{ m}$ . Due to the influence of near-surface anomalies, it is non-hyperbolic.

For the purpose of near-surface layer replacement, our goal is to replace the complex velocity layer (above  $600 \text{ m}$  in Figure 1a) with a homogeneous velocity, and here we choose this new

layer velocity to be 2000 *m/s*. The new velocity model is shown in Figure 1b and our target datum is now at  $z = 600\text{ m}$ .

Before showing the result from IFNSLR, let's first have a look at the result from NSLR wherein all new sources and receivers are still at the original locations as in the input data. As pointed out before, interpolation for complex data by itself is still a challenge, and until now no concrete conclusion exists regarding which particular interpolation scheme works best for complex near-surface situations. In this example, a 4D (time, azimuth, offset, CDP number) hybrid Radon reconstruction method (Verschuur et al., 2012) is used as our interpolation scheme in order to create sources at every 25 m. Next, we use the new velocity model, Figure 1b, to migrate it, and the result is shown in Figure 3a. The central shot gather after NSLR is shown in Figure 3b. NSLR removes the imprint due to the influence of the near-surface layer for those events below the datum but defocuses all events above the datum. Therefore, in Figure 3a only the data below the datum are meaningful, while the part above the datum carries distorted information. Comparing Figure 3 with Figure 2, two observations can be made: 1) the image after NSLR is poorer than the original image, and for the complex areas some uncertainties emerge, for instance the top part of the bump structure, which is located at  $(x = 5000\text{ m}, z = 800\text{ m})$ ; 2) the events in the shot gather look reasonable, but details are compromised, and the target event is not as smooth as one may expect. Although in theory NSLR should produce a final image with the same quality as Figure 2a, in reality interpolation for complex datasets is too challenging to provide a satisfying output.

IFNSLR avoids resorting to an interpolation scheme, and following the proposed IFNSLR workflow a new dataset can be obtained. In this new dataset, both sources and receivers are on a dense 25 *m* grid at the surface. This means that after IFNSLR, in terms of data volume, the new dataset is 8 times as big as the original sparse dataset. Figure 4a shows the migrated image with the replacement velocity model, and Figure 4b shows the central shot gather after IFNSLR. Comparing Figure 4a with Figure 2a, it can be clearly seen that below the datum, the results are

almost the same except at the left and right boundaries, which is due to edge effects in wavefield extrapolation. This supports our proposition that wavefield extrapolation is an information conservative manipulation as long as data volume expansion is allowed. Figure 4b also shows smooth reflection events after IFNSLR correction. This is indeed what we can expect, since without the influence of near-surface anomalies, the deep reflection events should be well behaved.

### **3D Field Data Example: IFNSLR for Stacking**

Although today stacking usually is no longer the ultimate processing step, it is still used as a quick QC tool. Similar to migration, stacking is also a sparse manipulation, but it maps data to a different sparse domain. For example, in 3D it maps 5-dimensional data,  $(s_x, s_y, g_x, g_y, t)$ , to a 3-dimensional  $(x, y, t)$  domain. In this example we are going to demonstrate IFNSLR for stacking.

We recently proposed 3D data-driven near-surface layer replacement with common focus point (CFP) operators to solve the complex near-surface problem (Sun et al., 2014; Sun and Verschuur, 2014, 2012a,b). In this method, CFP operators and replacement operators act as the original velocity model and the replacement velocity model in NSLR (Al-Ali and Verschuur, 2006), and the whole process can be done in a completely automatic manner. Since the original 3D field data are sparse, we also resorted to the earlier mentioned 4D hybrid Radon reconstruction method in our workflow, and the result is encouraging (Sun et al., 2014). Here we use IFNSLR to reprocess the same 3D field dataset.

For completeness, we first briefly reiterate some important information related to that 3D field dataset, and more details can be found in Sun et al. (2014). The dataset is from an area in the Middle East with a complex near-surface. The data acquisition geometry is a typical sparse 3D cross-spread geometry with an inline distance of 30 *m* and a crossline distance of 240 *m*. The

dataset covers an area of around 3 by 4 km, and there are about 2.4 million traces. The original CFP operators, which describe one-way wave propagation from the surface to the datum (Berkhout, 1997), are estimated by a self-adjustable input genetic algorithm (SAIGA) (Sun and Verschuur, 2012b, 2014), and the replacement operators are estimated by multi-variate linear regression (Sun and Verschuur, 2012a; Sun et al., 2014).

Figure 5 shows the time slice at the datum from the NMO-corrected and CMP-stacked 3D field dataset. Due to the influence of near-surface anomalies, there is a gray area (low amplitude area) in the center of the image. Three cross sections are selected for further illustration, as shown in Figures 6a, 7a and 8a. In this field dataset, the datum is at 1150 *ms*. NSLR correction of this 3D field data is discussed in detail in our previous publication (Sun et al., 2014), and here we only show results. Although results look encouraging (Figs. 6b, 7b and 8b) two effects can be observed: 1) more low frequency components emerge in the image; 2) event energy distribution seems a bit different from the original result. As we pointed out in our previous work (Sun et al., 2014), inaccurate interpolation could be one of the reasons that lead to these effects. With the new idea of IFNSLR we reprocess this 3D field dataset with the same CFP operators, but without data interpolation. In the new dataset both sources and receivers are reconstructed on a dense grid ( $\Delta s_x = \Delta g_x = 30\text{ m}$ ,  $\Delta s_y = \Delta g_y = 30\text{ m}$ ) at the surface. This means in terms of data volume the new dataset is 64 times as big as the original one. The final results are shown in Figures 6c, 7c, and 8c. For areas of interest below our datum ( $> 1150\text{ ms}$ ), the improvement is clearly visible. Furthermore, events confirmed by our a priori geological information have been singled out by arrows in Figures 6, 7 and 8, and the corrections by IFNSLR also meet our expectations. Overall, not only image resolution is improved considerably but also event energy distribution is very similar to the original one in the areas that are less distorted by the near-surface anomalies. Note that transmission amplitude changes are not corrected by either NSLR or IFNSLR, since the use of CFP operators only provides corrections in terms of kinematic effects. This 3D field data

example supports our point that for complex datasets interpolation is the weak link in the chain, and interpolation is not even needed as long as enough information is present in the original dataset and data volume expansion is allowed to preserve all this information.

## **CONCLUSIONS**

In summary, we have proposed the interpolation-free near-surface layer replacement, which allows near-surface layer replacement for complex and sparse datasets without resorting to data interpolation. We first pointed out that the final objective of the near-surface layer replacement is not to obtain a newly reconstructed wavefield, but to obtain a better final migration image. By realizing that 3D acquisition is usually designed for sufficient subsurface coverage, any interpolation scheme, which is not accurate enough, implies a danger of mixing artefacts with the true subsurface information, later degrading the final image. By introducing the concept of data volume expansion, we are capable of preserving information during the aliased wavefield extrapolation process. We successfully applied the interpolation-free near-surface layer replacement to two seismic datasets, one 2D complex synthetic dataset and one 3D field dataset, confirming the effectiveness of our proposed thinking.

## **ACKNOWLEDGMENTS**

The authors thank Saudi Aramco for permission to publish this paper, Dr. Tong Fei for his assistance on the 2D synthetic model building, and Dr. Mike Jervis for reviewing our paper.

## REFERENCES

- Al-Ali, M. N., and D. J. Verschuur, 2006, An integrated method for resolving the seismic complex near-surface problem: *Geophysical Prospecting*, **54**, 739–750.
- Alkhalifah T., and Bagaini C., 2006, Straight-rays redatuming: A fast and robust alternative to wave-equation-based datuming: *Geophysics*, **71**, U37 – U46.
- Berkhout, A. J., 1982, *Seismic migration, imaging of acoustic energy by wave field extrapolation, A: theoretical aspects*: Elsevier.
- , 1997, Pushing the limits of seismic imaging, part II: integration of prestack migration, velocity estimation and avo analysis: *Geophysics*, **62**, 954–969.
- Berryhill, J. R., 1979, Wave-equation datuming: *Geophysics*, **44**, 1329–1344.
- , 1984, Wave-equation datuming before stack: *Geophysics*, **49**, 2064–2066.
- Bevc, D., 1997, Flooding the topography: Wave-equation datuming of land data with rugged acquisition topography: *Geophysics*, **62**, 1558–1569.
- Biondi B., and Palacharla G., 1996, 3-D prestack migration of common-azimuth data: *Geophysics*, **61**, 1822 – 1832.
- Gardner, G. H. F., 1974, Formation velocity and density-The diagnostic basics for stratigraphic traps: *Geophysics*, **39**, 770–780.
- Gisolf, A., and D. J. Verschuur, 2010, *The principles of quantitative acoustical imaging*: EAGE publications bv.
- Keho, T. H., and P. G. Kelamis, 2012, Focus on land seismic technology: The near-surface challenge: *The Leading Edge*, **31**, 62–68.
- Kelamis, P. G., K. E. Erickson, D. J. Verschuur, and A. J. Berkhout, 2002, Velocity independent redatuming: A new approach to the near-surface problem in land seismic data processing: *The Leading Edge*, **21**, 730–735.

Lokshtanov D., and Lotsberg J. K., 2009, 3D wave-equation redatuming of common azimuth data: 79th Ann. Internat. Mtg., SEG, Soc. Expl. Geophys., Expanded abstracts, 2874 - 2878.

Marsden, D., 1993a, Static corrections - a review, part I: The Leading Edge, **12**, 43–48.

———, 1993b, Static corrections - a review, part II: The Leading Edge, **12**, 115–120.

———, 1993c, Static corrections - a review, part III: The Leading Edge, **12**, 210–216.

Sun, Y., and D. Verschuur, 2014, A self-adjustable input genetic algorithm for the near- surface problem in geophysics: Evolutionary Computation, IEEE Transactions on, **18**, 309–325.

Sun, Y., and D. J. Verschuur, 2012a, The solution of the near-surface problem by 3D near-surface layer replacement: 82nd Ann. Internat. Mtg., SEG, Expanded Abstracts, Soc. Expl. Geophys., Expanded abstracts, NS P1.5.

———, 2012b, Solution to the 3D complex near-surface problem by estimation of propagation operators: 74th Ann. Internat. Mtg., EAGE, Expanded Abstracts, Eur. Ass. of Geosc. and Eng., C016.

Sun, Y., E. Verschuur, and J. W. Vrolijk, 2014, Solving the complex near-surface problem using 3D data-driven near-surface layer replacement: Geophysical Prospecting, **62**, 491–506.

Taner, M. T., F. Koehler, and K. A. Alhilali, 1974, Estimation and correction of near-surface time anomalies: Geophysics, **39**, 441–463.

Tegtmeier S., Gisolf A., and Verschuur D. J., 2004, 3D sparse-data Kirchhoff redatuming: Geophysical Prospecting, **52**, 509 – 521.

Thorbecke, J. W., K. Wapenaar, and G. Swinnen, 2004, Design of one-way wavefield extrapolation operators, using smooth functions in WLSQ optimization: Geophysics, **69**, 1037–1045.

Verschuur, D. J., J. W. Vrolijk, and C. Tsingas, 2012, 4D reconstruction of wide azimuth (WAZ) data using sparse inversion of hybrid radon transforms: 82nd Ann. Internat. Mtg., SEG, Expanded Abstracts, Soc. Expl. Geophys., Expanded abstracts, SPIR 1.6.

Waters, K. H., 1987, Reflection seismology?-A tool for energy resource exploration: John Wiley and Sons.

Yilmaz, O., and D. Lucas, 1986, Prestack layer replacement: Geophysics, **51**, 1355–1369.



## LIST OF FIGURES

1 (a) 2D synthetic velocity model and (b) the corresponding replacement velocity model. Densities in both situations are related to the velocities by Gardner's Equation.

2 Original sparse data. (a) Migrated image using the true velocity model. (b) The central shot gather of the forward modelled data. The arrow points at the event reflected from the flat reflector at  $z = 2500m$ .

3 NSLR processed data. (a) Migrated image using the replacement velocity above the datum reflector. (b) The central shot gather of the NSLR processed data. The arrow points at the NSLR corrected reflection event from the flat reflector at  $z = 2500m$ , and this event corresponds to the event being pointed at by the arrow in Figure 2(a).

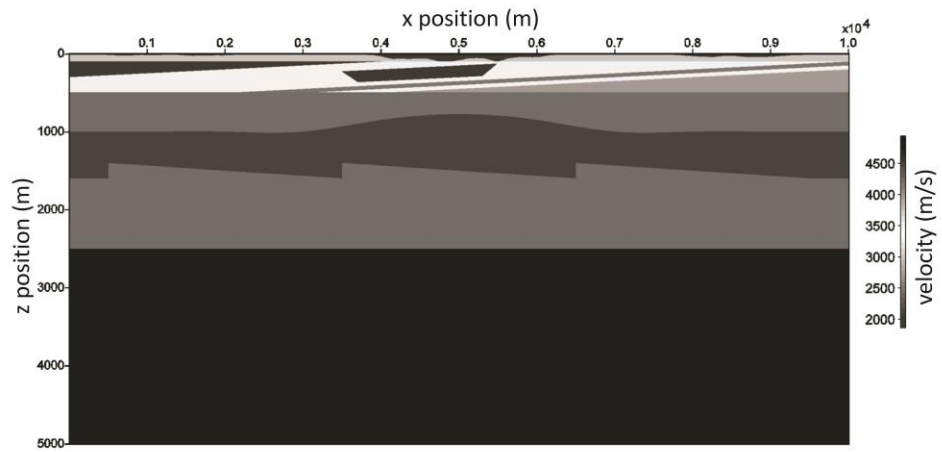
4 IFNSLR processed data. (a) Migrated image using the replacement velocity above the datum reflector. (b) The central shot gather of the IFNSLR processed data. The arrow points at the IFNSLR corrected reflection event from the flat reflector at  $z = 2500m$ , and this event corresponds to the event being pointed at by the arrow in Figure 2(a).

5 Time slice at the datum of normal move-out-corrected and CMP-stacked 3D field dataset. Dashed white lines indicate  $CMP-y = 3366, 3400, \text{ and } 3450$ .

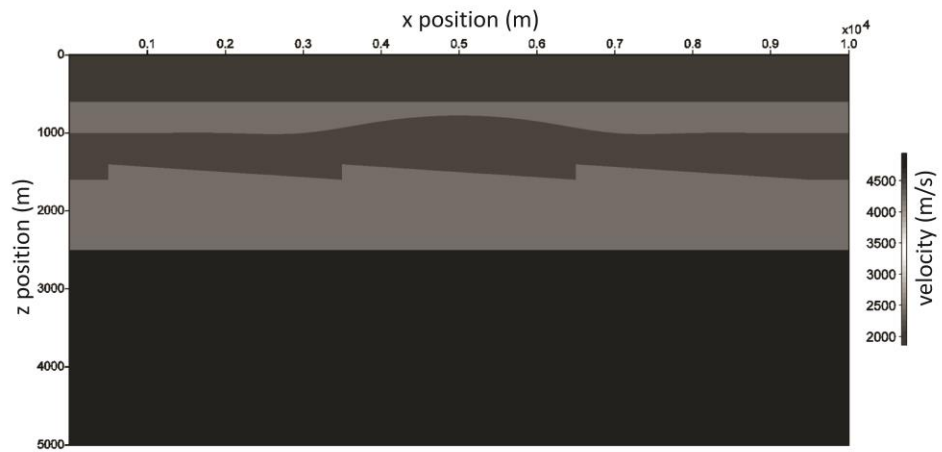
6 Stacking results at  $CMP-y = 3366$ . (a) Original data. (b) NSLR processed data. (c) IFNSLR processed data. Arrows point at the events confirmed by our a priori geological information.

7 Stacking results at  $CMP-y = 3400$ . (a) Original data. (b) NSLR processed data. (c) IFNSLR processed data. Arrows point at the events confirmed by our a priori geological information.

8 Stacking results at  $\text{CMP-y} = 3450$ . (a) Original data. (b) NSLR processed data. (c) IFNSLR processed data. Arrows point at the events confirmed by our a priori geological information.



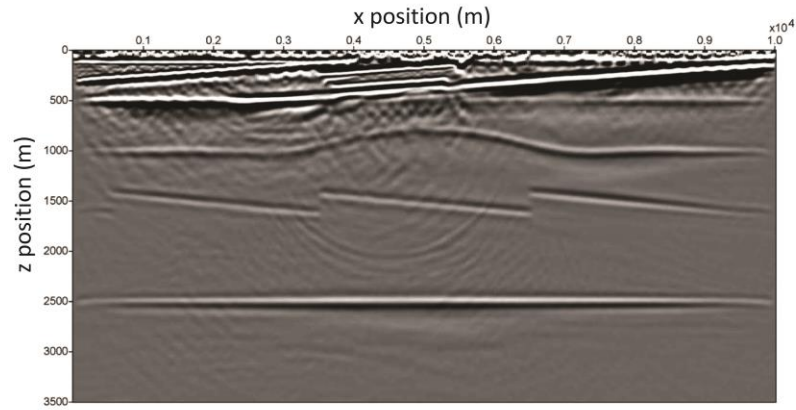
(a)



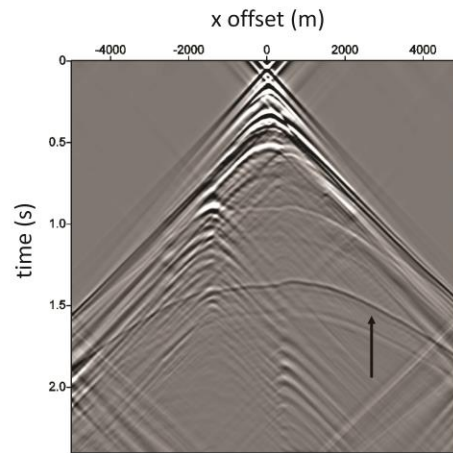
(b)

Figure 1: (a) 2D synthetic velocity model and (b) the corresponding replacement velocity model.

Densities in both situations are related to the velocities by Gardner's Equation.

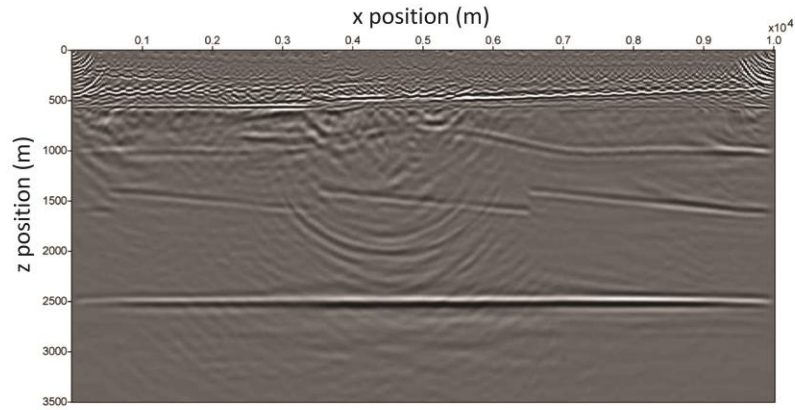


(a)

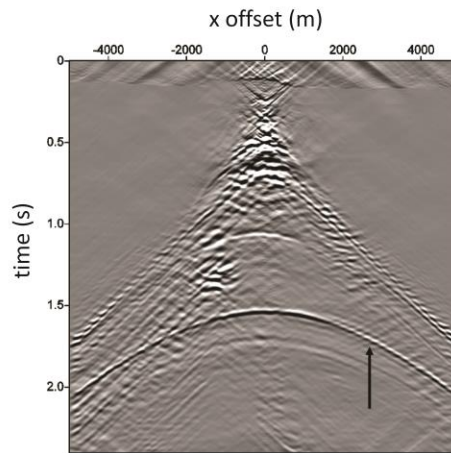


(b)

Figure 2: Original sparse data. (a) Migrated image using the true velocity model. (b) The central shot gather of the forward modelled data. The arrow points at the event reflected from the flat reflector at  $z = 2500m$ .

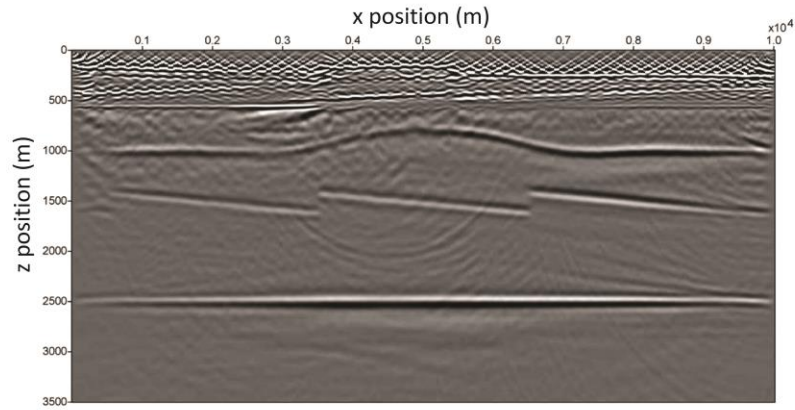


(a)

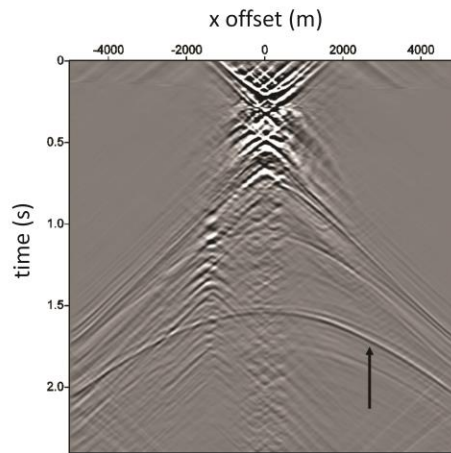


(b)

Figure 3: NSLR processed data. (a) Migrated image using the replacement velocity above the datum reflector. (b) The central shot gather of the NSLR processed data. The arrow points at the NSLR corrected reflection event from the flat reflector at  $z = 2500m$ , and this event corresponds to the event being pointed at by the arrow in Figure 2(a).



(a)



(b)

Figure 4: IFNSLR processed data. (a) Migrated image using the replacement velocity above the datum reflector. (b) The central shot gather of the IFNSLR processed data. The arrow points at the IFNSLR corrected reflection event from the flat reflector at  $z = 2500m$ , and this event corresponds to the event being pointed at by the arrow in Figure 2(a).

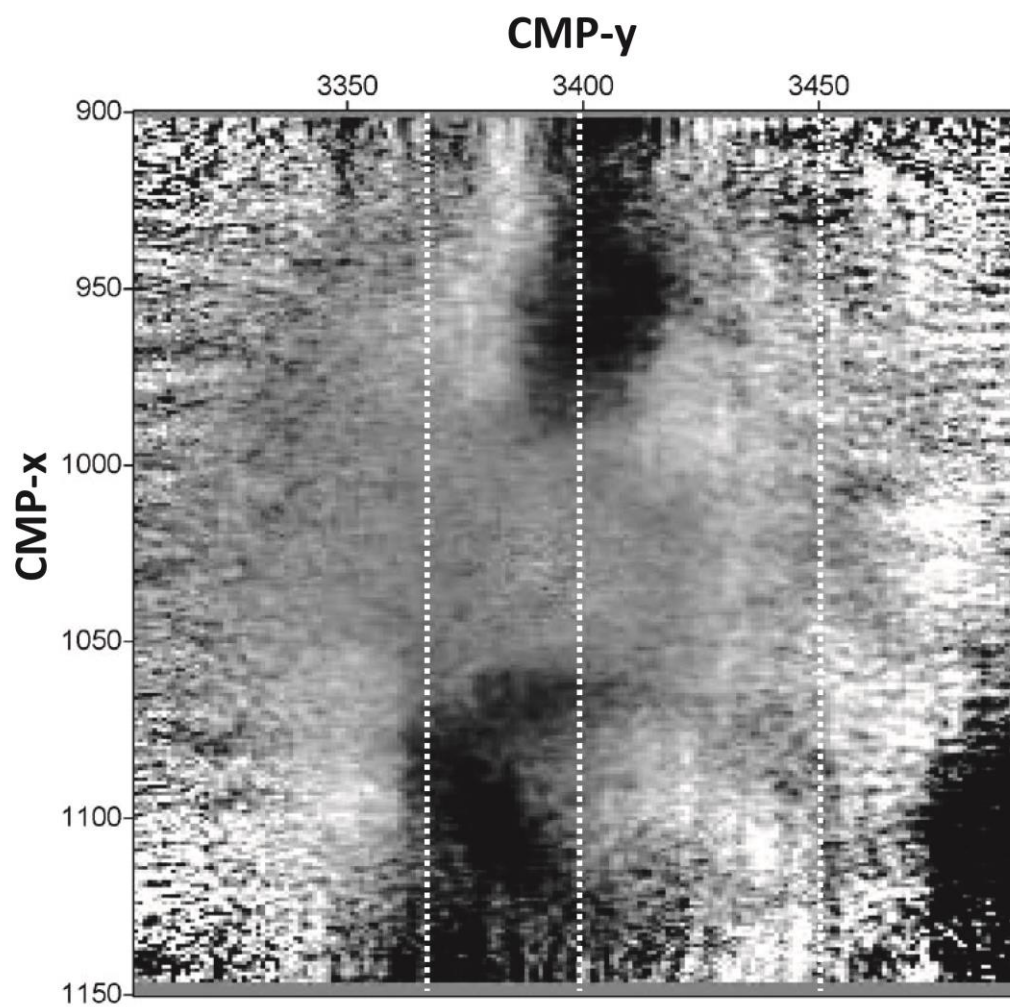
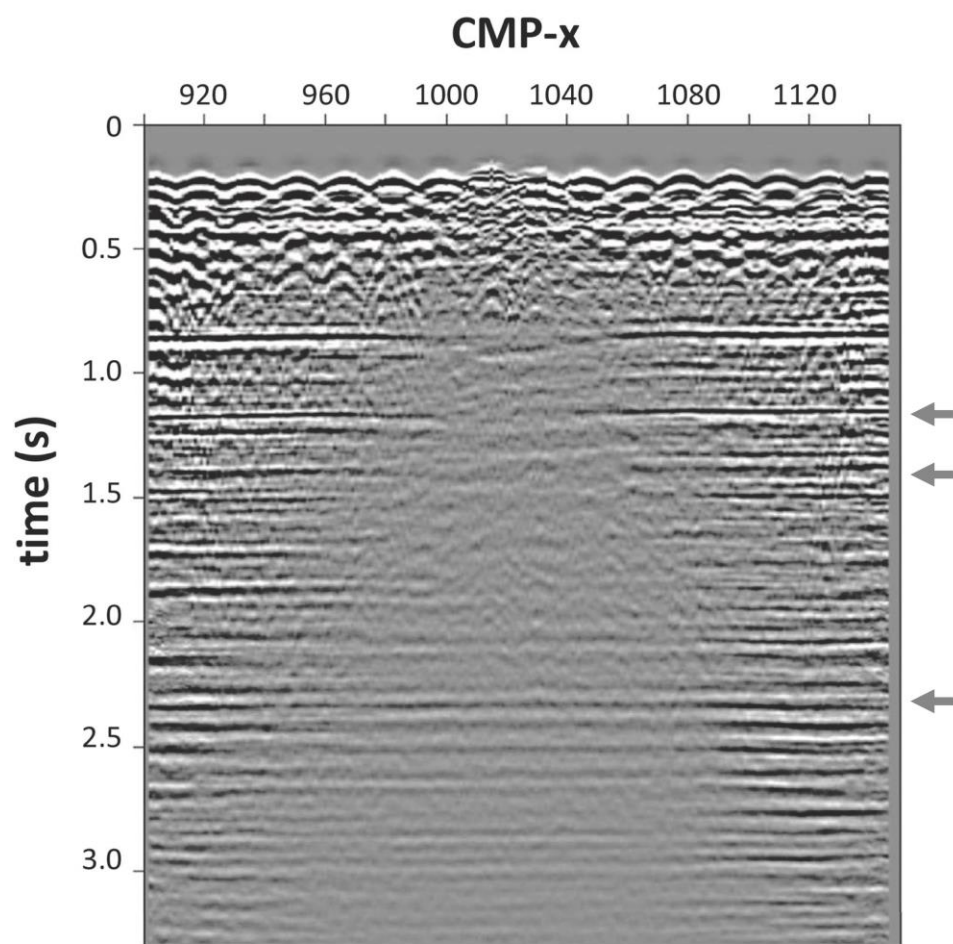
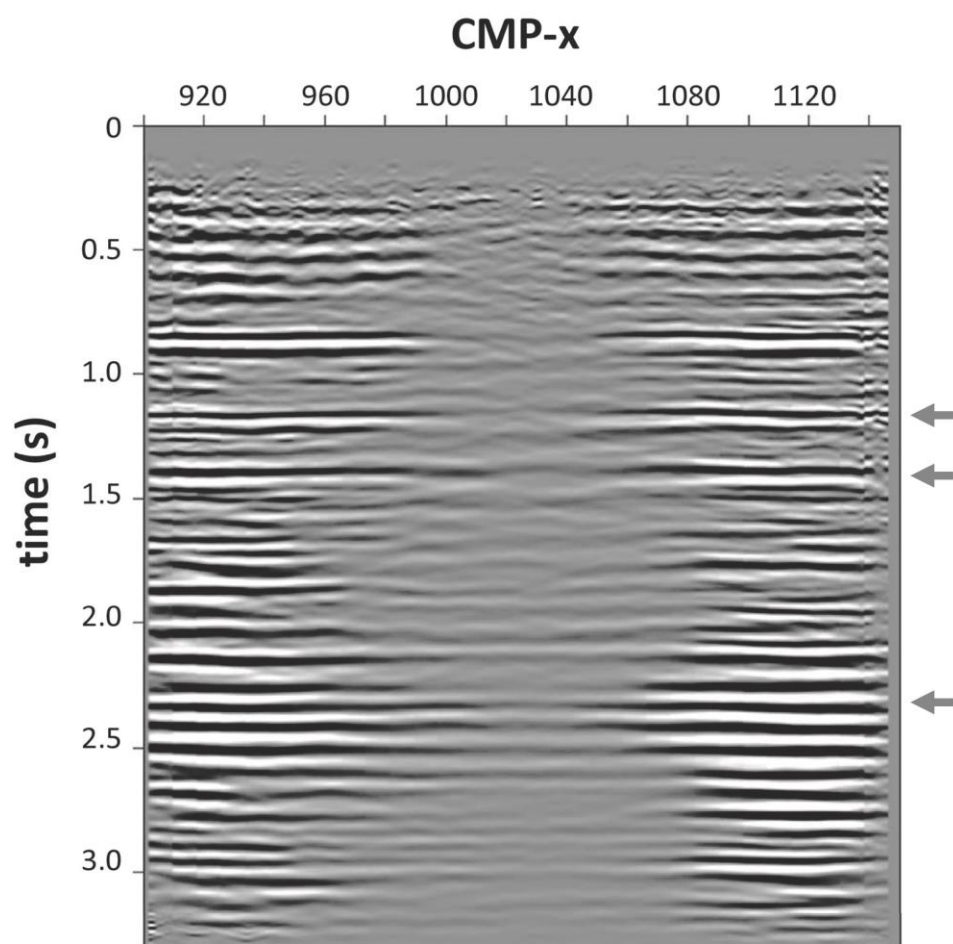


Figure 5: Time slice at the datum of normal move-out-corrected and CMP-stacked 3D field dataset. Dashed white lines indicate  $\text{CMP-y} = 3366, 3400,$  and  $3450$ .

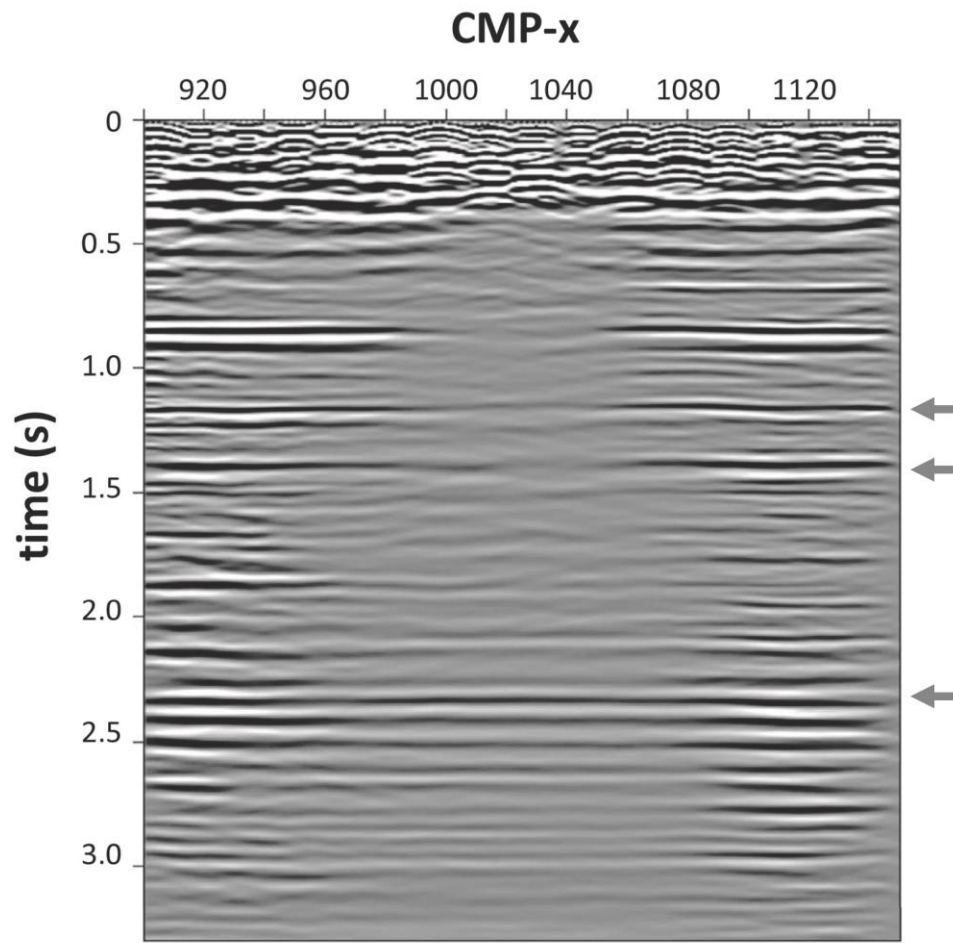


(a)



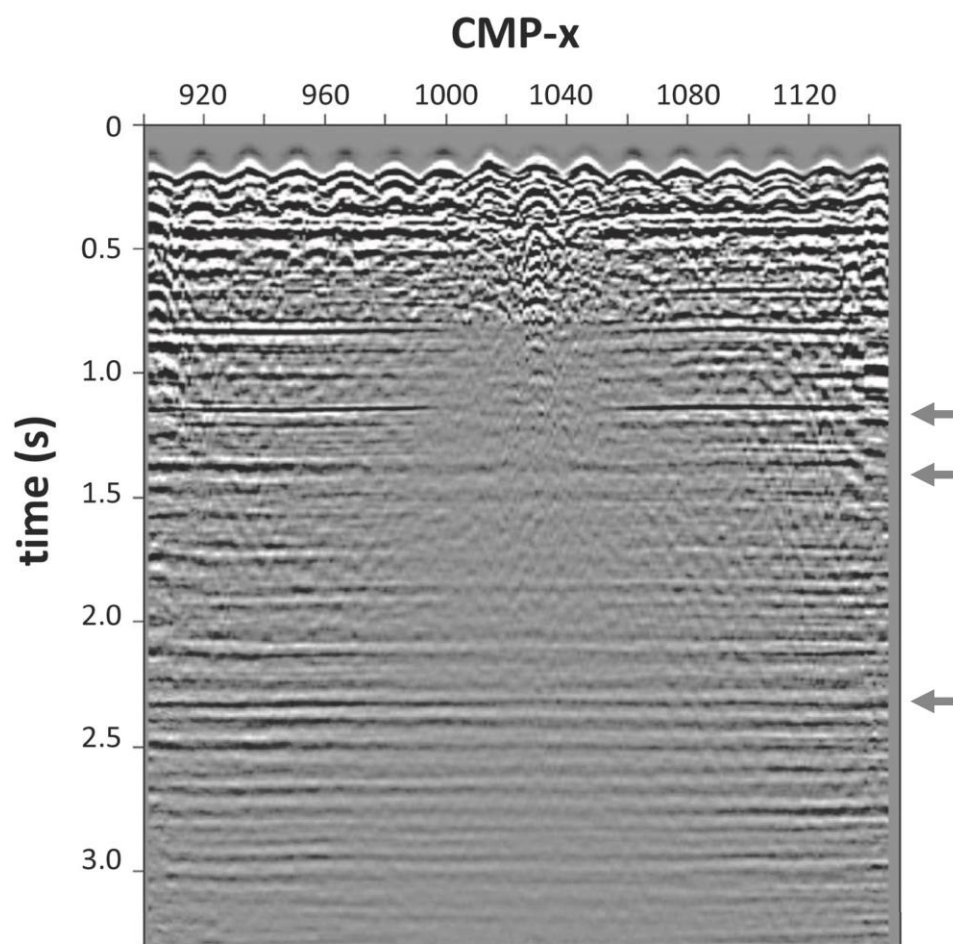


(b)

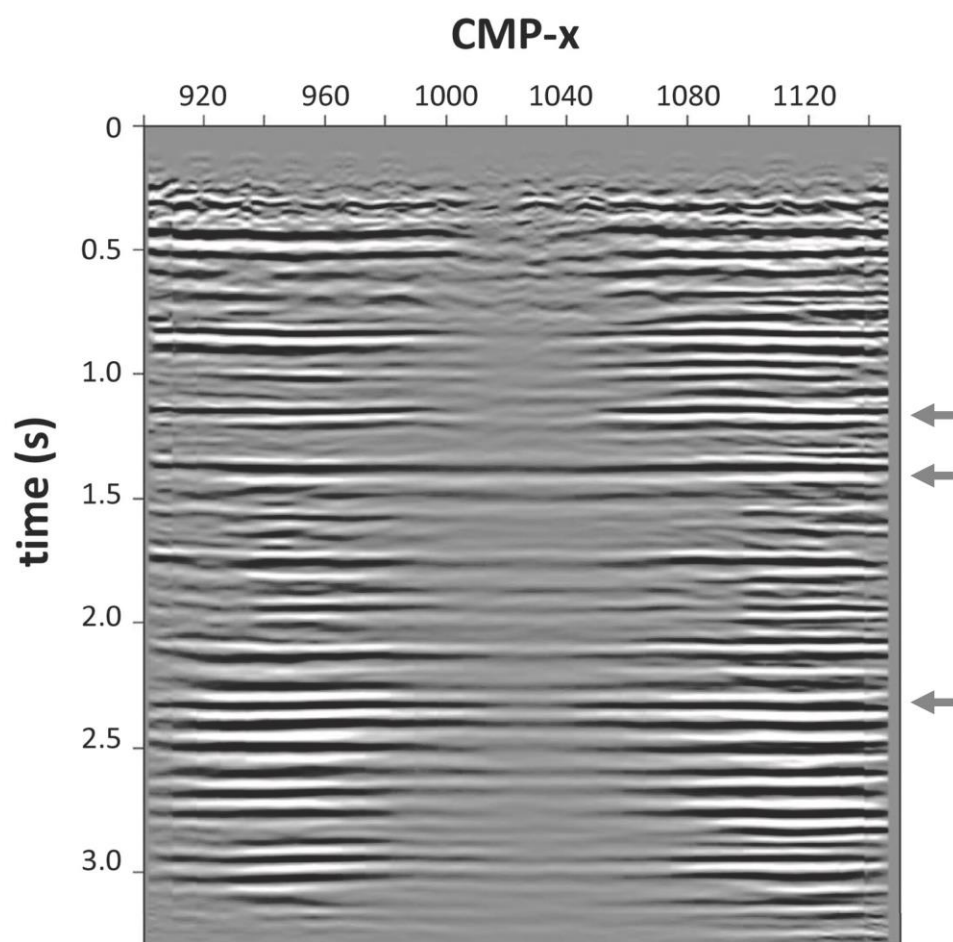


(c)

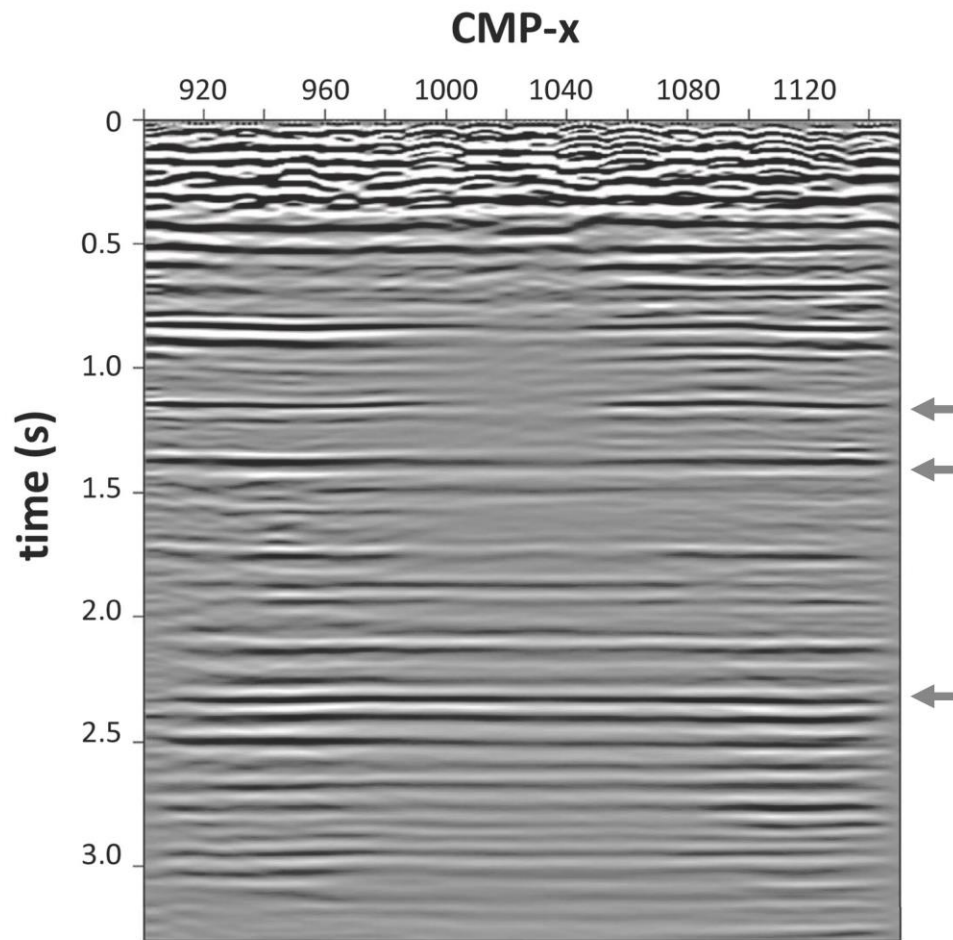
Figure 6: Stacking results at  $\text{CMP-y} = 3366$ . (a) Original data. (b) NSLR processed data. (c) IFNSLR processed data. Arrows point at the events confirmed by our a priori geological information.



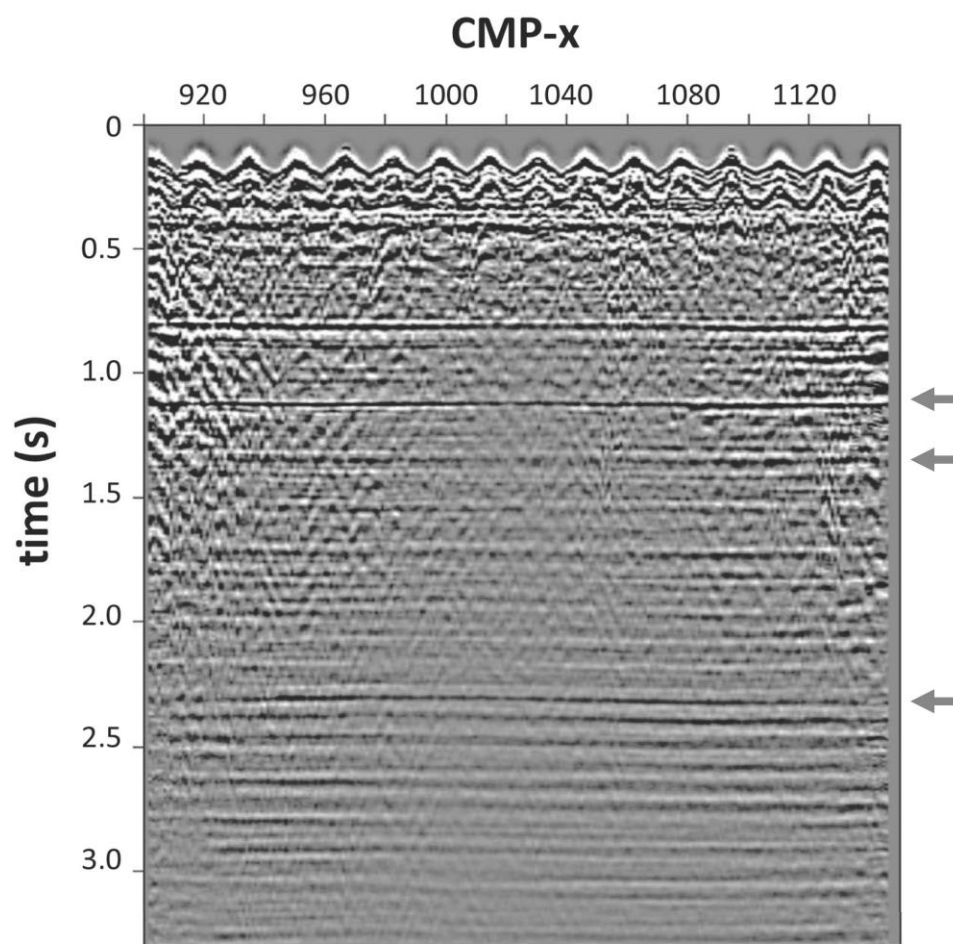
(a)



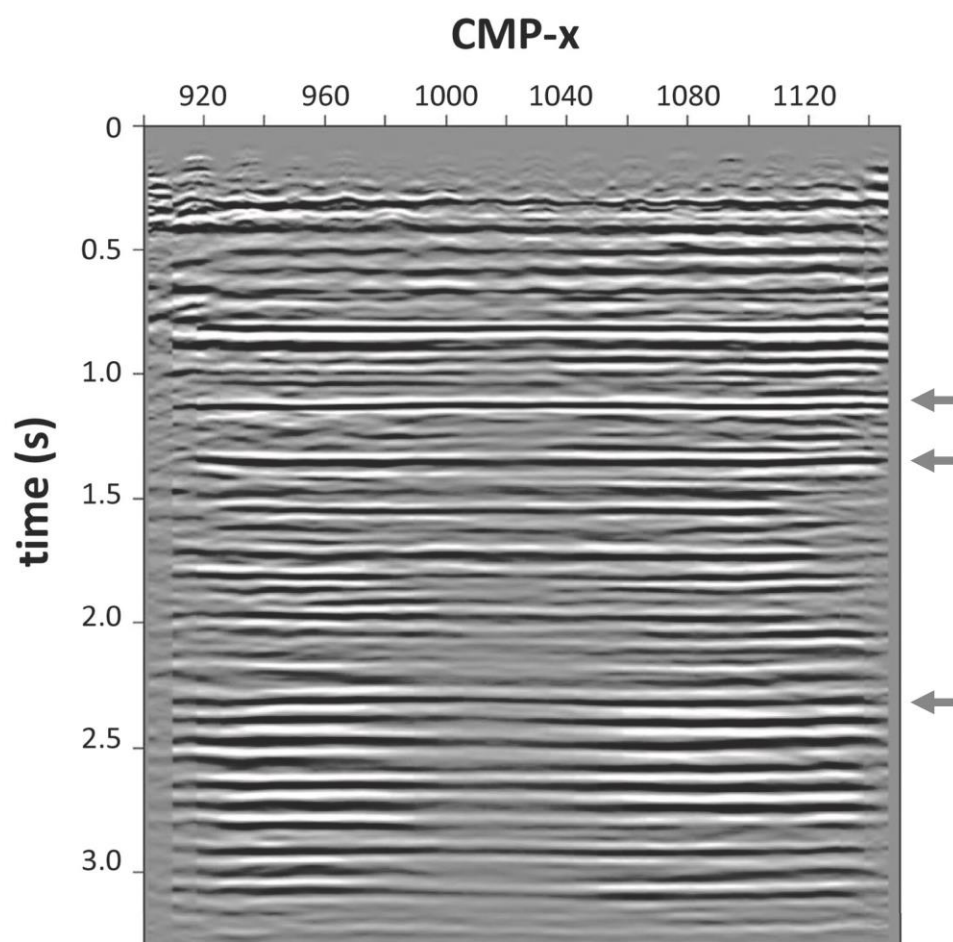
(b)



(c)  
 Figure 7: Stacking results at CMP-y = 3400. (a) Original data. (b) NSLR processed data. (c) IFNSLR processed data. Arrows point at the events confirmed by our a priori geological information.

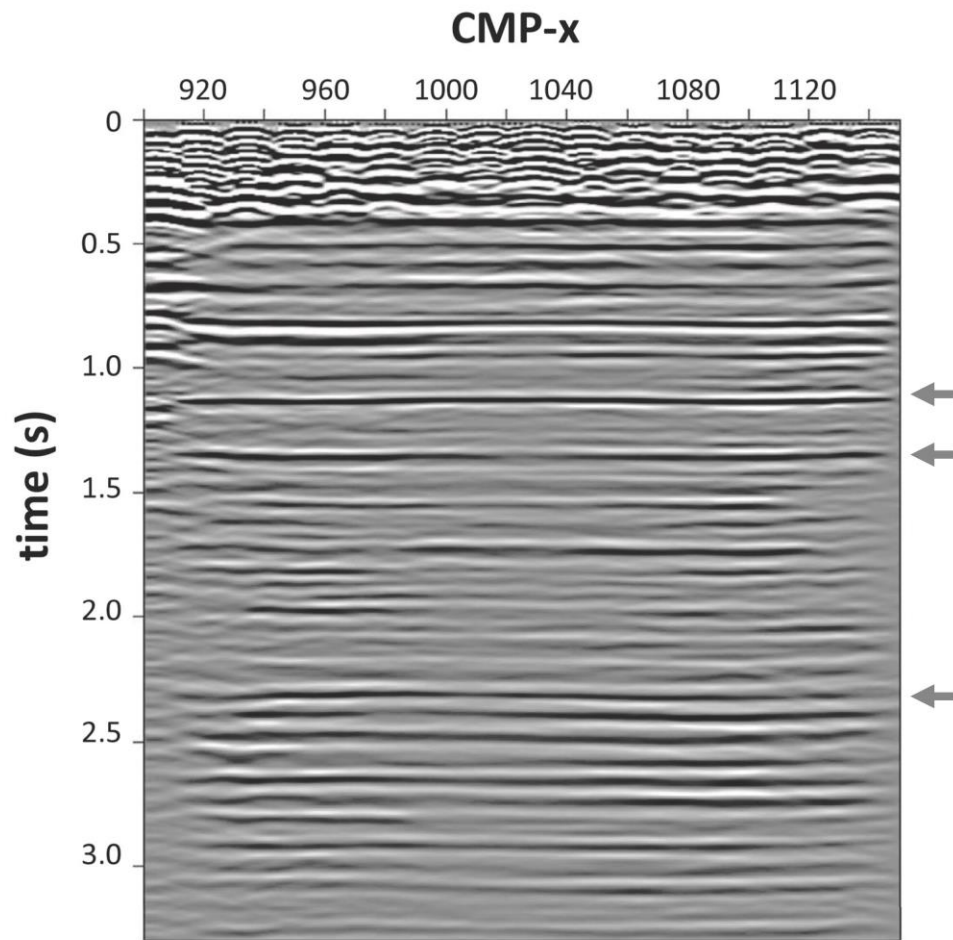


(a)



(b)





(c)  
Figure 8: Stacking results at CMP-y = 3450. (a) Original data. (b) NSLR processed data. (c) IFNSLR processed data. Arrows point at the events confirmed by our a priori geological information.